A New Upper Pliocene Palaeomagnetic Pole from Western Syria and a preliminary Polar Wander Curve of the Arabian Plate

Jamal Abou-Deeb

Department of Geology-Faculty of Sciences-University of Damascus-Syria

Received 31/05/2004
Accepted 30/11/2004

ABSTRACT

44 sites were sampled from the Upper Pliocene (βN^{b}_{2}) basaltic flows, from the western flank and the distant eastern flank of the Levant Fault in the Buqeia area NW of Tel Kalakh and west of Homs. Thermal demagnetization led to the identification of consistent directions of remanence in most sites. Normal, Reversed and Intermediate polarities are identified, with Reversed polarities dominating. The Intermediate polarity sites were excluded and the mean directions of the Reversed sites were reversed. The mean site direction of the 16 accepted sites from the western flank of the Levant Fault is 3.6º, 46.5º with α_{95}=7.0º, while the mean site direction of the 10 accepted sites from the eastern flank is 17.5º, 46.8º with α_{95}=2.6º. The overall mean direction of the 26 accepted sites in the western and eastern flanks is 9.0º, 46.9º with α_{95}=4.6º.

While the mean VGP of the 16 accepted sites from the western flank of the Levant Fault is 83.2º N, 188.3º E with α_{95}=7.0º, and the mean VGP of the 10 accepted sites from the eastern flank is 73.8º N, 145.6º E with α_{95}=2.6º. The overall mean VGP of the 26 accepted sites in the western and eastern flanks is 80.2º N, 162.4º E with α_{95}=4.8º.

The entire available palaeomagnetic pole data sources were consulted which resulted in collecting 51 poles from the Arabian plate, ranging in age from Precambrian to Quaternary. These poles were used to construct a preliminary polar wander curve, which will improve with the increase of the future results from Arabia.

Key words: Palaeomagnetism, Levant Fault, Upper Pliocene, Misiaf, Ghab, Syria, Lebanon

قطب مغنطيسي جديد من البليوسين الأعلى في غرب سورية ومنحنى تجول قطبي مقترح للصفيحة العربية

جمال أبو ديب

قسم الجيولوجيا - كلية العلوم - جامعة دمشق

تاريخ الإيداع 2004/05/31

قبل للنشر في 2004/11/30

الملخص

درست المغنطيسية القديمة لـ 44 موقعاً من بازلت البليوسين الأعلى من المنطقة الغربية والمنطقة الشرقية المحيطة بالفالق المشرقي في منطقة البقيعة الواقعة إلى الغرب من حمص. مكن التنظيف المغنطيسي للمغنطيسية القديمة من عزل مركبة مغنطيسية أولية في معظم المواقع. وتبين وجود جميع أنواع القطبية من نظامية، منعكسة ومتوسطة مع غلبة القطبية المنعكسة. وقد أهملت المواقع ذات القطبية المتوسطة وتم عكس اتجاهات المغنطيسية للمواقع المنعكسة. حسب متوسط الاتجاه المغنطيسي للمواقع المأخوذة من المنطقة الغربية (16 موقعاً) 3.6°, 46.5° و $\alpha_{95}=7.0^{\circ}$، في حين حسب الاتجاه للمواقع المأخوذة من المنطقة الشرقية (10 مواقع) 46.8° , 17.5° و $\alpha_{95}=2.6^{\circ}$، وكان المتوسط العام لجميع المواقع (26 موقعاً) 9.0°, 46.9° و $\alpha_{95}=4.6^{\circ}$.

حسب متوسط اتجاه القطب المغنطيسي للمواقع المأخوذة من المنطقة الغربية 83.2°N, 188.3° E و $\alpha_{95}=7.0^{\circ}$، في حين حسب متوسط اتجاه القطب للمواقع المأخوذة من المنطقة الشرقية 73.8° N, 145.6° E و $\alpha_{95}=2.6^{\circ}$، وكان المتوسط العام لاتجاه القطب لجميع المواقع 80.2° N, 162.4° E و $\alpha_{95}=4.8^{\circ}$.

جمعت جميع الأقطاب المغنطيسية (51 قطباً) من كل الدراسات المغنطيسية القديمة للصفيحة العربية وقد تراوحت أعمارها من ما قبل الكمبري حتى الرباعي واستخدمت في رسم منحنى تجول قطبي أولي للصفيحة العربية.

الكلمات المفتاحية: المغنطيسية القديمة، الفالق المشرقي، البليوسين الأعلى، مصياف، الغاب، سورية، لبنان.

Introduction and Regional Geology

The Levant transform fault system (Ponikarov, 1966; Best et al., 1993) - the northern-most extension of the Dead Sea transform fault system (Dubertret, 1970, Girdler, 1990) enters Syria from northern Lebanon, where it is called the Yemmunah Fault, and, in Syria, forms the Missiaf-Ghab fault system. That zone widens in the north to form the rhomb-shaped Missiaf-Ghab graben (Sigachev et al., 1995). The Yemmunah and Missiaf-Ghab fault systems are together widely regarded as the major seismic zone and the source of the volcanic activity in the area with a predicted left lateral displacement of about 20-25 km (Quennell, 1984; Trifonov et al., 1991). Although Butler et al. (1997) concluded that neither of these zones had been active during the past 5 Ma but that, during this time, seismic activity had mostly been associated with the Roum Fault that extends from south Lebanon through Beirut. The subaerial flood basalts of the Early Miocene, mostly ranging in age from 20 to 16 Ma ago, extended over most of southern Syria, Jordan and Saudi Arabia, but were absent along the Syrian coastal zone (Mouty et al., 1992). After a period of volcanic activity quiescence lasted tilll about 8 My ago an intensive volcanism commenced over most of Syria, but particularly along the rift margins in the south and the Levant transform fault margins in the north (Fig. 1). This phase of volcanism remained active into prehistoric time, for example, in the Karasu Valley, Southern Turkey, in the northernmost part of the rift (Capan et al., 1987) where ages range from 2 My to 0.4 My.

The studied area is mainly covered with the Upper Pliocene basaltic flows (βN^{b}_{2}) and the Quaternary sequences which are mostly consolidated sediments and are dominated by those of the Al Buqeia depression. The area is divided by the main N/S extending Levant Fault and many other faults, which are mainly trending N-S, NW-SE and NE-SW, but only the main faults are shown in Fig. 1.

Few palaeomagnetic studies were done (Van Dongen et al., (1967), Roperch and Bonhommet, (1986) and Abou-Deeb et al., (1999)). Three areas; 1- Sweida in the southern part of Syria, 2- Kisweh to the south of Damascus and, 3- the Homs-Shin basaltic flows west of Homs, were studied by Abou-Deeb et al., (1999) in order to widen the palaeomagnetic knowledge of the area. The results induced the author to undertake a new study of the Kisweh and the Homs-Shin basaltic flows. The later is the subject of this study that comprises the results of 44 sites, each comprising 6-7 samples, in Upper Pliocene (βN^{b}_{2}) basaltic flows, from the western flank and from the distant eastern flank of the Levant Fault. Generally, three sites were taken at separate locations within similar or identical exposures.

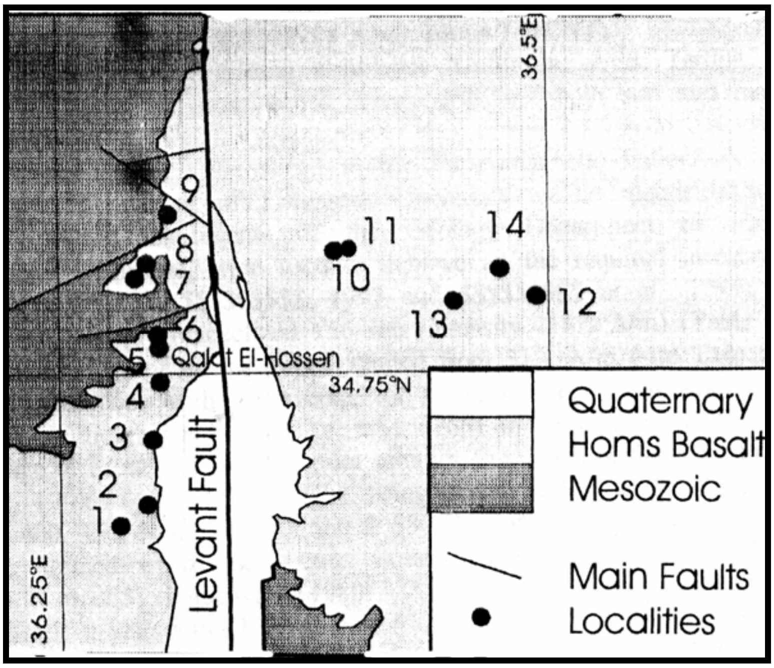

Fig. 1. Outline Geological Map of the studied area.

The sampling localities represent mostly 3 sites per volcanic unit. The main N/S Levant Fault is labelled, but, for clarity, the orientations of only a few relevant faults are marked. The fault trends are mainly N-S, NW-SE and NE-SW directions but only the main faults systems can be shown.
Numbers are as follows: 1=T31-T33, 2=T22-T24, 3=T4-T8, 4=T37-T39, 5=T19-T21, 6=T25-T28, 7=T40-T42, 8=T46-T48, 9=T43-T45, 10=T64-T66, 11=T67-T69, 12=T49-T51, 13=T52-T54, 14=T55-T57.

Sampling, Measurement and Treatment

Palaeomagnetic drilling techniques (Collinson, 1983; Tarling, 1983) were employed by using petrol driven drill and both sun and magnetic compasses were used for orientation. Then cores, 2.5 cm in diameter and 2.1 cm in height, were sliced in the Palaeomagnetic Laboratory of the Geology Department of Damascus University. The magnetometer and demagnetizing instruments of the Geology Department of Plymouth University, England, were used to achieve all the required measurements (Molyneux, 1971, Abou-Deeb, 1997 and Abou-Deeb et al., 1999). Apart from the strongly magnetized T56 site (intensity 116.5 A/m) (Table 1), the initial intensity of magnetization ranged from 31.4 A/m (site T44) to 0.59 A/m (site T66) with an average of 6.3±6.4 A/m. The site low-field susceptibilities ranged from 3.4 mSI (T66) to 71.1 mSI (T22) with an average of 31.8±17.1 A/m. 5 pilot samples from each of the main localities, T7.2, T20.6, T41.5, T54.2, T67.4, being treated at 100, 150, 200, 250, 300, 350, 400, 450, 500, 520, 540, 560 & 580ºC. Sample characteristic directions were defined where the vectors isolated had a mean angular deviation (*MAD*) of < 5º (Kirschvink, 1980). A site mean direction was considered further if it was defined by at least 5 samples with characteristic directions that agreed with an estimated 95% Probability cone of confidence of <15º (Fisher, 1953), that is the cone angle which is characterized by 95% probability that the true direction is located inside the cone is less than 15º. Alternating magnetic field demagnetization up to 100 mT was also undertaken on 5 samples from the same representative sites, but no reliable vectors could be isolated in any of these samples by using this technique. According to the study of the behavior of the pilot samples the rest of the samples were thermally demagnetized at 200, 300, 350, 400, & 420 ºC.

The magnetic susceptibility (Fig. 2) and intensity of magnetization (Fig. 3) of the pilot sample were studied in order to determine if any thermo-chemical changes had occurred to the magnetic minerals during heating. This will help in the extrapolation of the magnetic mineral that carries the magnetization of the rocks.

Fig. 2 shows variable changes in the magnetic susceptibility of all samples which indicate the presence of small amounts of other magnetic minerals and started to change, after heating to 50 °C with a major change started at 250 °C, to other minerals of higher susceptibility (like magnetite). While the decrease in the magnetic susceptibility after heating between 500 °C and 580 °C probably due to oxidation of magnetite to haematite.

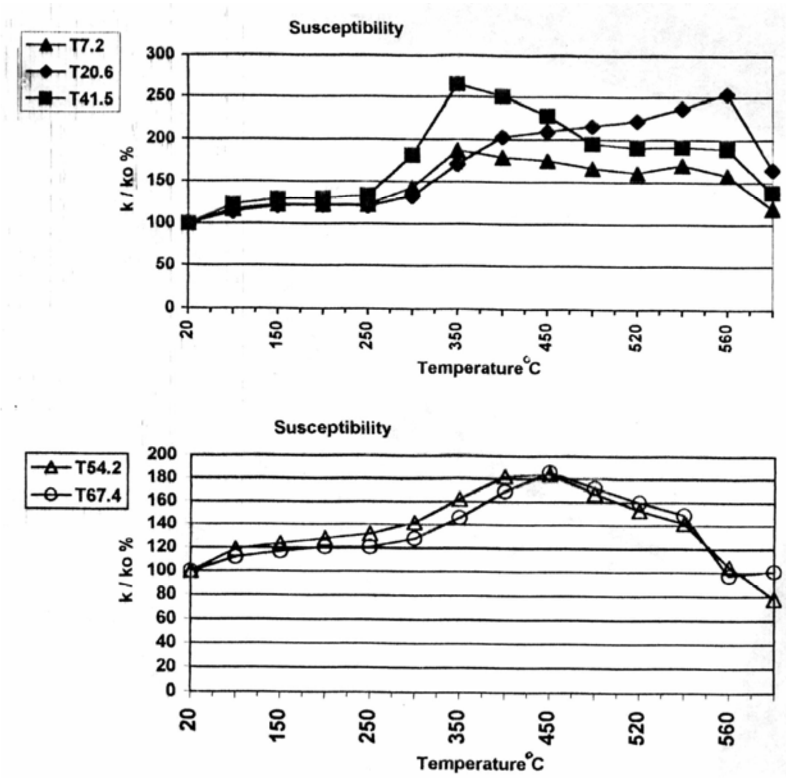

Fig. 2. Curves of normalized magnetic susceptibility of the pilot samples. Sample numbers and symbols are shown on the left side of figure.

In spite of the continuous decrease of the magnetic intensity of sample T54.2, the normalized magnetic intensity of all samples (Fig. 3) suggests that the main carrier of magnetization is magnetite.

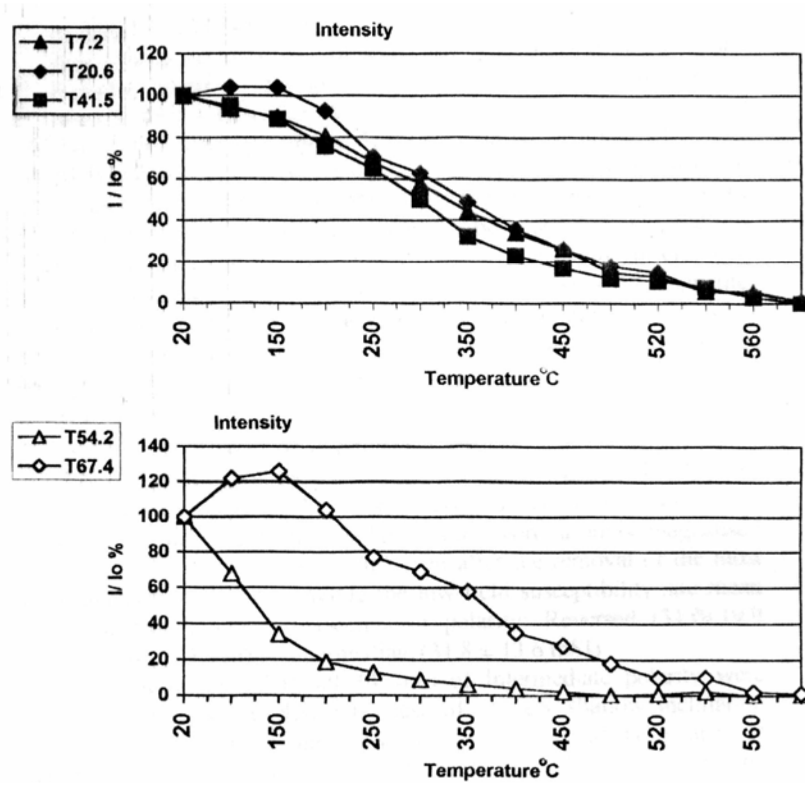

Fig. 3. Curves of normalized intensity of magnetization of the pilot samples. Sample numbers and symbols are shown on the left side of figure.

Results and Interpretations

In the majority of sites, the samples had well defined characteristic directions during thermal demagnetization, with their mean angular deviations (*MAD*) mostly being less than 3º. The main exceptions were in 2 sites (T4, T8) in which most samples *MAD*'s exceeded 5º; these sites were excluded from further directional analyses. In the remaining sites, the blocking temperature (Fig. 3) spectra suggested that the characteristic magnetic directions were carried by magnetite. Above about 250ºC, the low field susceptibility tended to increase (Fig. 2), but with no apparent effect on the linearity of the vector until approaching the Curie point of magnetite. A well defined site mean direction was isolated in most remaining sites, with the site mean precision estimate, α_{95} (Fisher, 1953), being <15º (Table 1). However, 1 site was rejected (T40) in which α_{95}>15º.

Normal (N), Reversed (R) and Intermediate (I) polarities were present (Table 1). According to the definitions (N = site virtual geomagnetic pole [VGP] latitude >50ºN; R = site VGP >50ºS; I = site VGP between 50ºN and 50ºS), the majority of the sites, 23, were of Reversed polarity, 4 were of Normal polarity and 14 were of Intermediate polarity. The mean site initial intensity of magnetization of the 23 Reversed polarity sites (3.9±3.1 A/m) was almost similar to that of the 4 Normally magnetised sites (4.1 ±1.1 A/m). The 14 sites of Intermediate polarity were more strongly magnetised and much more scattered (11.5±9.0 A/m) even after the removal of the most strongly magnetised site (T56). While the low-field susceptibility site mean values were almost similar, irrespective of polarity: Reversed (31.0±19.9 mSI), Normal (40.2±5.9 mSI), Intermediate (31.8 ± 13.6 mSI).

For calculating the VGP, all 14 sites of Intermediate polarity were ignored and site T38 was excluded because of its very shallow inclination (7.7º), which could have been caused by local movement and the polarity of the remaining 22 Reversed sites were reversed by 180º. Then the remaining 26 mean site vectors were northerly directed and have positive inclination. The mean site direction of the 16 accepted sites (T19-T24, T27, T31-T33, T37, T39, T42, T46-T48) from the western flank of the Levant Fault is 3.6º, 46.5º with α_{95}=7.0º (Table 2), while the mean site direction of the 10 accepted sites (T49-T51, T57, T64-T69) from the eastern flank is 17.5º, 46.8º with α_{95}=2.6º (Table 2). The overall mean direction of the 26 accepted sites from the western and eastern flanks is 9.0º, 46.9º with α_{95}=4.6º. Such a direction is consistent with that (5.6º, 49.9º), predicted for the Arabian plate some 10 Ma ago, after allowing for the opening of the Red Sea and using the African polar wander curve (Besse & Courtillot, 1991). This implies that the studied locality belongs to unrotated part of the Arabian Plate.

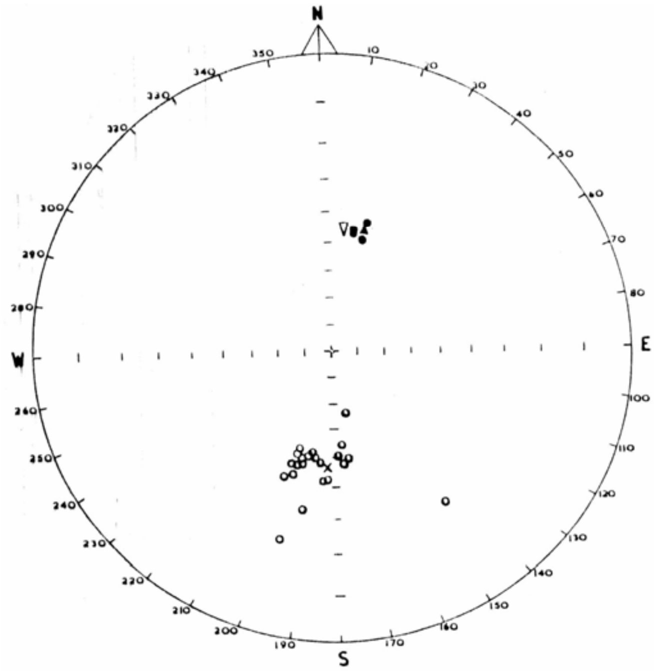

Fig. 4. Site mean directions after demagnetization plotted on an equal area projection. Positive (downward) inclinations are shown with solid circles and negative (upward) inclinations are shown with hollow circles. The solid triangle is the mean of the Positive inclinations and the (x) sign is the mean of the negative inclinations. The centre of the hollow inverted triangle is the overall mean site direction of the accepted sites after reversing the negative inclinations.

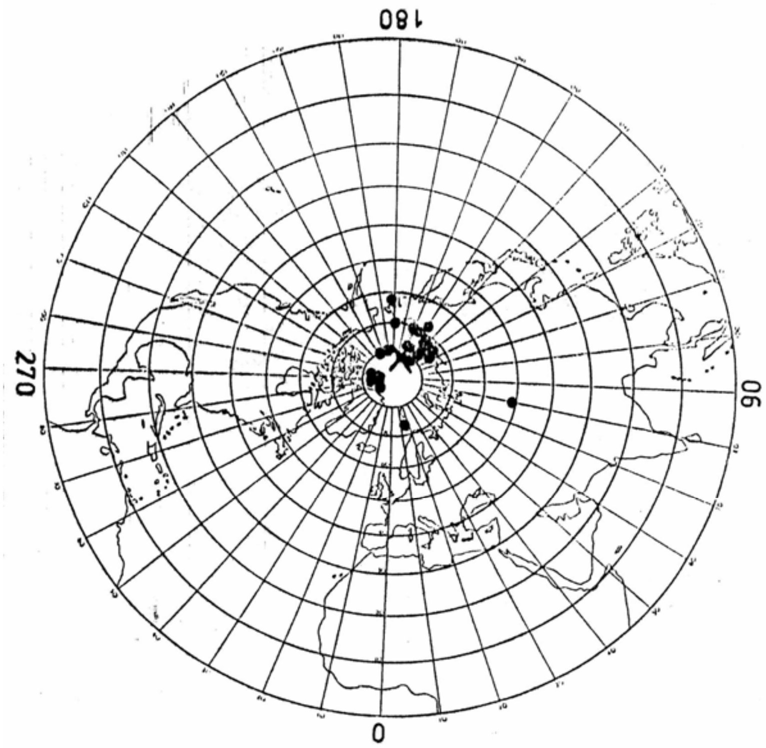

Fig. 5. Virtual Geomagnetic Poles derived from site mean directions plotted in Fig. 4. The overall mean of the VGP's is represented by the centre of the (X) sign.

While the mean VGP of the 16 accepted sites from the western flank of the Levant Fault is 83.2º N, 188.3º E with α_{95}=7.0º (Table 2), and the mean VGP of the 10 accepted sites from the eastern flank is 73.8º N, 145.6º with α_{95}=2.6º (Table 2). The overall mean VGP of the 26 accepted sites from the western and eastern flanks is 80.2º N, 162.4º with α_{95}=4.8º

Table 1. Site Mean Intensity, Susceptibility, Direction of Remanence and pole position. The number of samples per site, with a vector defined with a mean angular deviation (*MAD*) less than 5º (Kirshvink, 1980) is N, compared with the total number of samples collected, n. The mean initial intensity of magnetization (Int.) is in units of A/m and the mean susceptibility (Susc.) are in mSI units. The site mean directions (Declination, Decl. and Inclination, Incl.) are listed with the estimates of precision, *k*, and 95% Probability, α_{95} (Fisher, 1953). The VGP latitude (Lat.) and longitude (long.) are calculated for each site. The polarity (Pol.) of each site is Normal (N), when the virtual geomagnetic pole latitude is greater than 50ºN, Reversed (R), when greater than 50ºS, and Intermediate (I) when between these two limits. "Scattered" sites (S) are when there are fewer than 5 samples with *MAD* < 5º or when the site precision, α_{95}, exceeds 15º.

Site	N/n	Int. A/m	Susc. mSI	Decl.	Incl.	k	α_{95}	Lat.	Long.	Pol.
Eastern Flank										
Ain-Kut										
T64	6/6	1.69±0.37	13.86±4.98	199.4	-43.1	1915	1.5	-70.6	331.3	R
T65	6/6	1.03±0.12	6.17±0.43	199.0	-45.9	1760	1.6	-72.1	325.9	R
T66	6/6	0.59±0.06	3.44±0.34	194.2	-50.2	727	2.5	-77.5	320.4	R
T67	5/6	1.58±0.26	27.17±3.60	199.4	-51.6	574	3.2	-73.7	309.9	R
T68	6/6	1.60±0.23	24.87±4.98	202.4	-40.8	108	6.5	-67.4	330.8	R
T69	6/6	2.46±0.68	40.33±2.26	199.7	-44.9	440	3.2	-71.2	327.2	R
Sufer										
T49	6/6	3.86±0.41	33.52±2.04	18.1	46.9	618	2.7	73.2	144.9	N
T50	6/6	3.83±0.42	40.63±2.90	12.2	45.8	379	3.4	77.1	159.3	N
T51	6/6	3.13±0.30	47.90±1.77	12.2	46.5	643	2.6	77.5	157.3	N
T52	6/6	11.87±3.80	48.43±1.82	314.7	-1.7	659	2.6	34.7	276.3	I
T53	6/6	19.55±3.20	50.98±6.23	308.8	0.2	452	3.2	31.0	281.9	I
T54	5/6	20.15±0.98	39.81±1.71	254.7	-1.2	1126	2.3	-12.9	314.9	I
T55	6/6	4.95±1.70	40.66±3.95	256.1	-8.0	112	6..4	-13.7	311.1	I
T56	6/6	116.50±5.09	37.36±2.49	257.5	-17.5	325	3.7	-15.3	306.1	I
T57	5/6	5.75±1.95	38.91±6.65	17.8	52.4	122	6.9	75.1	128.3	N
Western flank										
Marmarita										
T40	5/6	7.43±1.08	36.58±2.27	Scattered		21	17.0	scattered		S
T41	5/6	5.30±0.19	8.61±1.76	112.7	-62.2	1671	1.9	-38.5	157.5	I
T42	6/6	2.20±0.80	6.83±1.12	170.5	-66.9	134	5.8	-73.7	193.8	R
T43	6/6	21.47±3.29	30.87±1.45	73.9	4.3	161	5.3	14.4	133.9	I
T44	6/6	31.38±4.87	28.09±0.97	57.4	5.4	423	3.3	28.0	144.0	I
T45	6/6	12.20±1.47	21.89±3.58	33.4	16.3	300	3.9	49.6	159.3	I
T46	5/6	1.86±0.45	63.40±2.14	175.8	-54.1	165	6.0	-86.5	125.2	R
T47	5/6	2.27±0.26	49.71±1.52	182.5	-43.1	318	4.3	-80.0	22.9	R
T48	6/6	1.87±0.17	53.61±2.18	185.4	-42.4	483	3.1	-78.7	10.5	R
Qalat El-Hossen										

T19	6/6	5.18±0.32	21.20±1.67	195.5	-49.2	944	2.2	-76.2	321.9	R
T20	5/6	2.94±0.10	6.75±0.71	189.9	-49.9	1319	2.1	-80.8	329.9	R
T21	6/6	3.09±0.14	10.57±2.00	187.7	-48.1	1375	1.8	-81.4	344.8	R
T25	4/7	4.70±1.36	37.96±3.48	132.1	-18.3	43	14.2	-39.5	107.9	I
T26	6/6	4.39±0.64	44.10±2.97	131.0	-13.2	308	3.8	-37.0	106.1	I
T27	6/6	2.86±0.86	32.05±1.34	145.0	-24.1	178	5	-51.4	100.0	R
T37	6/7	8.37±1.63	20.00±6.22	192.8	-32.5	162	4.8	-69.4	359.3	R
T38	5/6	12.41±1.82	22.46±2.40	209.0	-7.7	54	10.5	-49.1	348.7	R
T39	6/6	11.34±1.86	22.69±2.01	195.6	-21.2	240	4.5	-62.3	1.6	R
Tel Kalakh										
T4		2.81±0.48	32.42±0.99	Undefined				undefined		S
T5	5/6	5.40±1.89	31.87±6.74	120.3	-59.9	121	7.0	-43.3	152.3	I
T6	4/6	3.41±1.40	11.32±5.11	109.6	-56.1	175	7.0	-34.1	150.4	I
T7	5/6	4.20±0.67	13.39±2.63	115.6	-54.7	231	5.0	-38.2	146.6	I
T8		4.45±0.43	7.86±0.44	undefined				undefined		S
T22	6/6	2.73±0.36	71.05±3.01	175.8	-48.6	467	3.1	-83.7	72.2	R
T23	6/6	3.96±1.45	57.19±11.02	177.5	-51.4	1057	2.1	-86.6	75.8	R
T24	6/6	5.93±1.04	65.42±4.41	173.7	-49.6	1091	2.0	-83.2	89.6	R
T31	6/6	3.76±0.27	30.20±2.18	190.9	-51.2	77	7.7	-80.4	320.4	R
T32	7/7	3.86±0.96	33.46±1.77	197.5	-47.5	347	3.2	-73.9	323.6	R
T33	7/7	5.54±1.16	31.71±0.78	198.2	-49.6	45	9.1	-74.1	316.8	R

Table 2. The mean directions and VGP positions and parameters of the accepted sites in the western and eastern flanks of the Levant Fault after reversing the negative inclinations. Symbols as in Table 1.

No of Site	No. on samples	Decl.	Incl.	k	α_{95}	Lat.	Long.	α_{95}	Pol.
Mean of the accepted sites in the western flank (T19-T24, T27, T31-T33, T37, T39, T42, T46-T48)									
16	96	3.6	46.5	29	7.0	83.2	188.3	7.0	Reverse
Mean of the accepted sites in the eastern flank (T49-T51, T57, T64-T69)									
10	58	17.5	46.8	352	2.6	73.75	145.6	2.6	Mixed
Overall mean of the accepted sites (T19-T24, T27, T31-T33, T37, T39, T42, T46-T51, T57, T64-T69)									
26	154	9.0	46.9	40	4.6	80.2	162.4	4.8	Mixed

Arabian plate palaeomagnetic poles

All the available palaeomagnetic pole data sources were consulted (The Norwegian Geological Society Internet pole listing, Palaeomagnetic directions and pole positions compiled by M.W. McElhinny (1968, 1971, 1972, 1977), palaeomagnetic database compiled by J. Piper (1988), Palaeomagnetism and Plate tectonic written by M.W. McElhinny (1973) and all the available papers) in order to collect all the data. This resulted in collecting 51 poles, including the present result, (Table 3) from the Arabian plate, and ranging in age from Precambrian to Quaternary. No strict criterion on the validity of the data was applied due to the low number of the geographically widely dispersed studies, with the hope that the future increase of the palaeomagnetic studies will enforce such criterion in order to get a more reliable polar wander curve for the Arabian plate.

Table 4 gives the pole means of the different geological ages. Quaternary (Q) and Pliocene-Pleistocene (T_p- Q_p) poles resulted from one pole each. While Pliocene to Lower Cretaceous poles were chosen according to good grouping of poles i.e. ($\alpha_{95} < 20^o$). Also Ordovician to Upper Cambrian (O – **Єu),** Cambrian (Є), and two Lower Cambrian **(Єl)** and Precambrian (PC) poles resulted from one pole. Those poles which resulted from only one pole were used separately due to the difference in absolute age. Fig. 6 shows the polar wander curve of the poles shown in Table 4, but the Precambrian pole was not drawn because it looks very strange, which may have resulted from local movement.

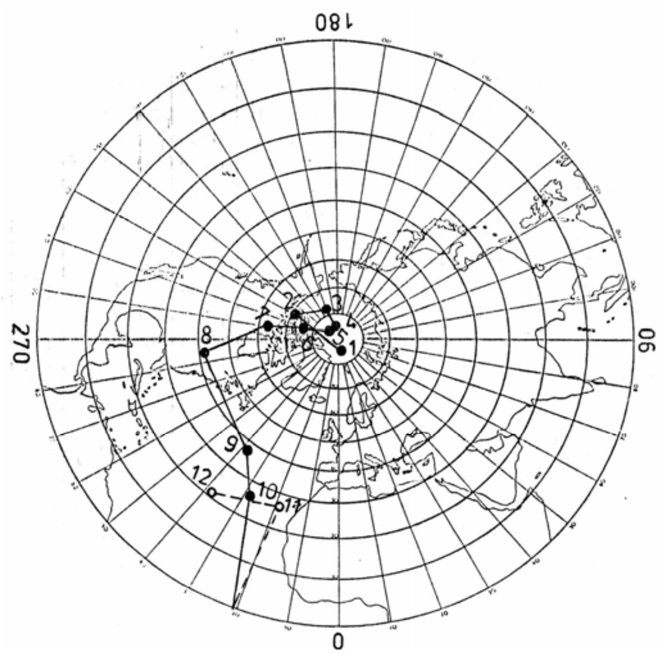

Fig. 6. Polar wander curve of the Arabian plate. Pole numbers are as in column two of Table 4. The hollow circles are on the southern hemisphere

Table 3. Summary of all the available Arabian plate poles. Symbols are: Si = No. of sites, Sa = No. of samples, α_{95}= is the cone angle which is characterized by 95% probability that the true direction is located inside the cone. dp, dm=error parameters on the pole position. t = thermal treatment, a = a. f. current treatment. Q=Quaternary, Qp= Pleistocene, Tp = Pliocene, Tm=Miocene, To=Oligocene, Te=Eocene, Ku=Upper Cretaceous, Kl=Lower Cretaceous, J=Jurassic, Ju=Upper Jurassic, Jl=Lower Jurassic, Tr=Triassic, P=Permian, O=Ordovician, Є=Cambrian, Єu=Upper Cambrian, Єl=Lower Cambrian, PC = Precambrian. The top symbol or numbers in column 3 are the geological age of rock while the bottom number is the age of magnetization.

Pole No.	Rock unit and Coordinates	Age (My)	Si (Sa) & treatment	Pole Position Lat.	Pole Position Long.	α_{95} or dp, dm	Polarity	Reference
1	Holocene Basalts, Sweida, Syria 32.6 N, 36.3 E	Q	14 (86) t	85.6N	20.4 E	11.6	M	Abou-Deeb et al. (1999)
2	Pleistocene basalt lava, Jordan 31.43 N, 35.79 E	Tp-Qp 0-2	4 (25) a	73.8N	241.3 E	4.9	M	Sallomy and Krs (1980)
3	Volcanics, group1, Palestine 33.4 N, 35.5 E	Tp-Qp 0-5	5(30) a	77.7 N	200.1 E	20.4	M	Nur & Helsley (1971)
4	Pliocene basalts, Lebanon	Tp 2-4		83.4 N	203.6 E	7.7		Gregore et al. (1974)
5	Upper Pliocene basalts, Lebanon 33.4 N, 35.8 E	Tp 2-4	15(78) a	88 N	169 E	7.7	M	Gregore et al. (1974)
6	Hatrurim formation, Palestine 31.5 N, 35.3 E	Tp 2-5	18 (119) a	82.9 N	135.6 E	5.2		Ron & Kolodny (1992)
7	Volcanics, group2, Palestine 33.5 N, 35.5 E	Tp 2-15	3 (46) a	32 N	313.0 E	13.0	M	Nur & Helsley (1971)
8	Syrian Basalts, Syria 34.8 N, 35.8 E	Tp 2-5	2 (7)	73.0	251.0 E	10,3	R	Van Dongen et al. (1967)
9	Aden Volcanics, Yemen 13.0 N, 45.0 E	Tp 5	11(-) a, r	85 N	298 E		M	Tarling et al. (1967)
10	U-Pliocene Basalts, W. of Homs, Syria 34.7 N, 36.3 E	Tp 5-6	26 (154) t	80.2 N	162.4 E	4.8	M	Present study
11	U-Pliocene Basalts, W. of Homs, Syria 34.4 N, 36.2 E	Tp 5-6	9 (52) t	80.3 N	195.8 E	11.7	M	Abou-Deeb et al. (1999)
12	Little Aden Volcanics, Yemen 13.0 N, 45.0 E	Tp 5-6	5(16) a	78 N	147 E		R	Tarling et al. (1967)
13	Yemen Volcanics, Yemen 13.0 N, 45.0 E	Tm 5-10	33 (124) a	83.5 N	292.3 E	6.3		Tarling et al. (1967)
14	Aden Volcanics, Yemen 12.8 N, 45.0 E	Tm 5-10	12 (54) a	83.0 N	310.0 E	3.0		Irving & Tarling (1961)

15	Neocene Basalts, Jordan 32.2 N, 36.5 E	Tm 5-23	1 (6) a	76.2 N	99.1 E	2.1		Sallomy and Krs (1980)
16	Jabel Khariz Volcanics, Yemen 13.0 N, 45.0 E	Tm 10	14(47) a, r	77 N	309 E		M	Tarling et al. (1967)
17	Mount Timna igneous rocks, Palestine 29.8 N, 34.9 E	610-620 10-20	6 (79) a, r	83.6 N	223.2 E	4.4		Marcos et al. (1993)
18	Middle Miocene basalts, Kisweh, Syria 33.2 N, 36.1 E	Tm 16-20	23 (134) t	74.6N	196.0 E	4.4	M	Abou-Deeb et al. (1999)
19	Basalts, Saudi Arabia	Tm 18-20		86.3 N	199.5 E	5.2		Yousif & Beckmann (1981)
20	Miocene Volcanics, Syria 33.25 N, 36.25 E	Tm 19.5	23(108) a, r	75 N	220 E	5,9	M	Roperch and Bonhommet (1986)
21	Hudyadah Volcanics, Yemen 15.0 N, 44.0 E	Tm 23.3	7(38) t	78.5 N	182.8 E	12.5	N	Abou-Deeb (2004)
22	Masirah ophiolite, Oman 20.4 N, 58.8 E	145-152 20-40	-(18) t	78.0 N	240.0 E	5.9	N	Gnos & Perrin (1996)
23	Upper lavas, Madrakah, Saudi Arabia	To 24-30		80.9 N	247.9 E	10.1		Yousif & Beckmann (1981)
24	Sana'a Volcanics, Yemen 15.2 N, 44.1 E	To 29.6	8(46) t	76.6 N	251.3 E	9.4	R	Abou-Deeb et al. (2002)
25	As Sarat Volcanics, Saudi Arabia	To-Tm 29-31	42 (-)	78.8 N	247.8 E	4.3	M	Kellogg & Reynolds (1983)
26	Lower lavas, Madrakah, Saudi Arabia	Te 35-45		68 N	242.8 E	4.2		Yousif & Beckmann (1981)
27	Masirah ophiolite, Oman 20.4 N, 58.8 E	145-152 50-60	-(15) t	56.0 N	282.0 E	8.5	M	Gnos & Perrin (1996)
28	Usfan formation, Saudi Arabia	Kl 65-74		62.9 N	231.2 E	13.2		Yousif & Beckmann (1981)
29	Cretaceous Lavas (1), Palestine 32.5 N, 35.0 E	Ku 65-89	2(15) a	41.6 N	264.2 E	5.4	N	Helsley & Nur (1970)
30	Cretaceous sediments, Palestine 31.0 N, 35.0 E	K 65-146	4(--) a	77.1 N	250.8 E	19.6		Freund & Tarling (1979)
31	Oman ophiolite unit V3, Oman 24.2 N, 53.6 E	K 74-87	-(27) a	66.4 N	231.7 E	3.7	N	Perrin et al. (1994)
32	Oman ophiolite unit V2, Oman 24.2 N, 53.5 E	K 88-94	-(18) a	11.0 N	314.4 E	4.9	N	Perrin et al. (1994)

33	Wadi Kadir gabbro, Oman 22.8 N, 58.6 E	K 93-98	16 (45) a	60.5 N	285.0 E	7.6	N	Luyendyk & Day (1982)
34	Sheeted dyke, Samail ophiolite, Oman 22.8 N, 58.6 E	K 93-98	28 (202) a	75.6 N	256.5 E	7.0	M	Luyendyk et al. (1982)
35	Oman ophiolite unit V1, Oman 24.2 N, 53.5 E	K 94-105	-(35) a	41.8 N	284.4 E	2.7	N	Perrin et al. (1994)
36	Cretaceous Lavas (2), Palestine 31.0 N, 35.0 E	Kl 97-146	3(22) a	52.8 N	265.1 E	8.6	N	Helsley & Nur (1970)
37	Volcanics and sediments, Lebanon 34.0 N, 36.0 E	Kl 97-146	5(15) a	38 N	282 E	8.9	N	Van Dongen et al. (1967)
38	Essexite Laccolith, Palestine 30.6 N, 34.9 E	J- K 97-157	3(--) a	48.3 N	265.6 E	6.8, 13.6	N	Freund & Tarling (1979)
39	Volcanics, Mount Harmon, Lebanon	Kl 113-119		4.3 N	301.5 E	15.5		Ron (1987)
40	Neocomian basalts, Lebanon 34.0 N, 35.6 E	Kl 132-146	9(47) a	25 N	285.0 E	9.0	M	Gregore et al. (1974)
41	Masirah ophiolite, Oman 20.4 N, 58.8 E	J 145-152	-(29) t	3 N	271.0 E	9.7	N	Gnos & Perrin (1996)
42	Kimeridgian basalts, Lebanon 34.0 N, 35.8 E	Ju 146-156	8(52) a	2 N	114 E	10.6	R	Gregore et al. (1974)
43	Basalts and tuffs, Lebanon 34.1 N, 35.8 E	Ju 152-155	6(20) a	1 N	120 E	4.3	R	Van Dongen et al. (1967)
44	Ardon formation, Palestine 30.6 N, 34.8 E	Ju 157-208	5(--) a	74.8 N	248.7 E	15.6	M	Freund & Tarling (1979)
45	Saharonim formation, Palestine 30.6 N, 34.9 E	Tr 208-245	3(--) a	48.6 N	179.7 E			Freund & Tarling (1979)
46	SHDI sediments, Saudi Arabia 24.0 N, 45.0 E	P - Tr 241-248	- (16) t	53.2 N	250.2 E	15.9		Torq et al. (1997)
47	Red sandstones, Jordan 29.7 N, 35.3 E	O - Єu 470-505	(20) a, t	37 N	323 E	7.5	M	Burek (1969)
48	Diorite Stock, Saudi Arabia 21.7 N, 43.7 E	Є 505-545	1 (12) a, t	25.8 N	332.2 E	11.8		Kellogg & Beckmann (1983)
49	Dykes, Jordan 29.5 N, 35.1 E	Єl 525-545	2(12) t	26.0 S	341.0 E	8.6		Sallomy and Krs (1980)
50	Mirbat sandstone, Oman 17.1 N, 54.8 E	Єl 530-560	2 (10) t	23.3 S	321.8 E	7.2	N	Kempf et al. (2000)
51	Arfan Formation, Saudi Arabia 21.3 N, 43.7 E	PC 590-620	12 (63) a, t	77.4 N	297.9 E	10.8		Kellogg & Beckmann (1983)

Table 4. Gives the mean of the Arabian poles given in Table 3. Column one gives the age as in Table 3, column two gives the pole number on Fig. 6 and column three gives the numbers of the used poles to calculate the mean as given in Table 3.

Age	Pole number on Fig. 6	Used Poles	Lat. (N)	Long. (E)	α_{95}
Q	1	1	85.6	20.4	11.6
Tp-Qp	2	2	73.8	241.3	4.9
Tp-Qp	3	3	77.7	200.1	20.4
Tp	4	4-6, 8-12	84.2	193.5	5.7
Tm	5	13- 21	85.2	220.4	6.7
To-Tm	6	22- 26	76.5	245.5	4.8
Ku	7	27-31, 33-34	64.4	260.2	11.8
Kl	8	36- 38, 40	41.4	275.8	16.8
O - **€u**	9	47	37.0	323.0	7.5
€	10	48	25.8	332.2	11.8
€l	11	49	26.0 S	341.0	8.6
€l	12	50	23.3 S	321.8	7.2
PC	13	51	77.4	297.9	10.8

Acknowledgements

The author is grateful to the University of Damascus for the financial support of the project of this research. Thanks are due to the officials of the Department of Geology of the University of Plymouth - England, for making facilities available for measurement and analysis as part of the concordat between the Universities of Plymouth and Damascus. Thanks are particularly due to Prof. D. H. Tarling for making this project a reality and Dr. Tony Morris for his suggestions and help during the work in the Palaeomagnetism Laboratory.

REFERENCES

Abou -Deeb, J. M. (1997). Studies of some magnetic and physical properties of some Quaternary - Recent basaltic rocks (Jabal Al-Arab, Syria). Damascus University Journal (Basic Sciences), Vol. 13, No. 1, pp. 131-151.

Abou-Deeb, J .M., Otaki, M. M., Tarling, D. H. and Abdeldayem, A. L. (1999). A palaeomagnetic study of Syrian volcanic rocks of Miocene to Recent age. Geofisica Internacional, 38, (1) 17-26.

Abou-Deeb, J., Tarling D.H., and Abdeldayem A. L. (2002). Preliminary Palaeomagnetic Stratigraphy of the Tertiary Yemen Volcanics. Geofisica Internacional, Vol. 41, No. 1, 37-47.

Abou -Deeb, J. M. (2004). Study of palaeomagnetism and some magnetic and physical properties of some Tertiary igneous rocks between Sana'a and Al-Hudyadah region. (Republic of Yemen). Damascus University Journal, (Basic Sciences), (accepted for publication).

Besse, J. and Courtillot, V. (1991). Revised and synthetic apparent polar wander paths of the African, Eurasian, North American and Indian Plates, and true polar wander since 200 Ma. J. Geophys. Res., 96, 4029-4050.

Best, J., Barazangi, M., Al-Saad, D., Sawaf, T., and Gebran, A. (1993). Continental margin evolution of the northern Arabian platform in Syria. Amer. Assoc. Petrol. Geol. Bull., 77, 173-193.

Burek, P. J. (1969). Device for chemical demagnetization of red beds. Jour. Geophys. Res., 74, 6710-6712.

Butler, R. W.H., Spencer, S. and Griffith H.M. (1997). Transcurrent fault activity on the Dead Sea Transform in Lebanon and its implications for plate tectonics and seismic hazard. Jour. Geol. Soc., London, 154, 757-760.

Capan, U.Z., Vidal, Ph., and Cantagrel, J.M. (1987). K-Ar, Nd, Sr and Pb isotopic study of Quaternary volcanism in Karasu valley (Hatay), N-end of the Dead Sea Rift zone in SE-Turkey. Yerbilimleri, 14, 165-178.

Collinson, D.W. (1983). Methods and Techniques in Rock Magnetism and Palaeomagnetism, Chapman & Hall, London, pp.503.

Dubertret, L. (1970). Review of the structural geology of Red Sea and surrounding areas; Royal Society of London Philosophical Transaction, ser. A, 267, 9-20.

Fisher, R.A., (1953). Dispersion on a sphere. Proc. Roy. Soc., A217, 295-305.

Freund, R., and Tarling, D. H. (1979). Preliminary Mesozoic palaeomagnetic results from Israel and interferences for a microplate structure in the Lebanon. Tectonophysics, 60, 189-205.

Girdler, R. W. (1990). The Dead Sea transform fault system. Tectonophysics, 180, 1-13.

Gnos, E., and Perrin, M. (1996). Formation and evolution of the Masirah Ophiolite constrained by palaeomagnetic study of volcanic rocks. Tectonophysics, 253, 53-64.

Gregore, C. B., Mertzman, S., Nairn, A. E. M. and Negendank, J. (1974). The palaeomagnetism of some Mesozoic and Cenozoic volcanic rocks from the Lebanon. Tectonophysics, 21, 375-395.

Helsely, C. E. Nur, A. (1970). The palaeomagnetism of Cretaceous rocks from Israel. Earth Planet. Sci. Letters, 8, 403-410.

Irving, E. and Tarling D. H. (1961). The palaeomagnetism of Aden Volcanics. J. Geophys. Res., 66, 549-556.

Kellogg, K. S. and Beckmann, G. E. T. (1983). Palaeomagnetic investigations of Upper Proterozoic rocks in the eastern Arabian Shield, Kingdom of Saudi Arabia. Bull. Fac. Earth Sci. King Abdullaziz Univ. 6, 483-500.

Kellogg, K. S. and Rynolds, R. L. (1983). Opening of the Red Sea: constraints from a palaeomagnetic study of the As Sarat volcanic field, south- western Saudi Arabia. Geophys. J. Roy. Astro. Soc., 74, 649-665.

Kempf, O., Kellerhals, P., Lowrie, W., and Mattar, A. (2000). Palaeomagnetic direction in Late Precambrian glaciomarine sediments of the Mirbat Sandstone Formation, Oman. Earth Planet. Sci. Letters, 175, 181-190.

Kirschvink, J.L. (1980). The least-squares line and plane and the analysis of palaeomagnetic data. Geophys. J. R. astr. Soc., 62, 699-718.

Luyendyk, B. P., Laws, B. R., Day, R., and Collinson, T. R. (1982). Palaeomagnetism of the Samail Ophiolite, Oman 1. The sheeted dike complex at Ibra. J. Geophys. Res., 87, 10883-10902.

Luyendyk, B. P., and Day, R. (1982). Palaeomagnetism of the Samail Ophiolite, Oman 2. The Wadi Kadir gabbro section. J. Geophys. Res., 87, 10903-10917.

McElhinny, M.W. (1968). Notes on progress in geophysics: Palaeomagnetic directions and positions-IX. Geophys. J. R. ast. Soc., 16, 207-224.

McElhinny, M.W. (1971). Notes on progress in geophysics: Palaeomagnetic directions and positions-XII. Geophys. J. R. ast. Soc., 27, 237-257.

McElhinny, M.W. (1972). Notes on progress in geophysics: Palaeomagnetic directions and positions-XIII. Geophys. J. R. ast. Soc., 30, 281-293.

McElhinny, M.W. and Cowley, J. A. (1977). Notes on progress in geophysics: Palaeomagnetic directions and positions-XIV. Geophys. J. R. ast. Soc., 49, 313-356.

McElhinny, M.W. (1973). Palaeomagnetism and plate Tectonics. Cambridge University Press, 358.

Marcos, S., Ron, H., Matthews, A., Beyth, M., and Navon, O. (1993). Chemical remnant magnetism related to the Dead Sea Rift: evidence from Precambrian igneous rocks of Mount Timna, southern Israel. J. Geophys. Res., 98, 16001-16012.

Molyneux, L.M. (1971). A complete results magnetometer for measuring the remnant magnetization of rocks. Geophys. J. R. astr. Soc., 24, 429-433.

Mouty, M., Delaloye, M., Fontignie, D., Piskin, O., and Wagner, J. (1992). The volcanic activity in Syria and Lebanon between Jurassic and the Actual. Schweiz. Mineral. Petrogr. Mitt., 72, 91-105.

Nur, A. and Helsely, C. E. (1971). Palaeomagnetism of Tertiary and Recent lavas of Israel. Earth Planet. Sci. Letters, 10, 375-379.

Ponikarov, V.P. (1966).(Editor). Explanatory notes on the Geological Map of Syria: Scale 1:1,000,000, Ministry of Industry, Damascus, Syria.

Perrin, M., Prevot, M., and Bonere, F. (1994). Rotation of the Oman ophiolite and initial location of the ridge in the hotspot reference frame. Tectonophysics, 229, 31-42.

Piper, J.D.A. (1988). Palaeomagnetic database. Open University Press,

Quennell, A.M. (1984). The Western Arabian rift system. In: Dixon, J.E. & Robertson, A.H.F. (eds.) The Geological Evolution of the Eastern Mediterranean. Geological Society, London. Special Publication, 17, 775-788.

Ron, H. (1987). Deformation along the Yemmunah, the resraining bend of the Dead Sea transform, palaeomagnetic data and kinematic implication. Tectonics, 6, 653-666.

Ron, H. and Kolodny, Y. (1992). Palaeomagnetic and rock magnetic study of Combustion metamorphic rocks in Israel. J. Geophys. Res., 97, 6927-6939.

Roperch, P. and Bonhommet, N. (1986). Palaeomagnetism of Miocene volcanism from South Syria, J. Geophys., 59, 98-102.

Sallomy, J., and Krs, M. (1980). A palaeomagnetic study of some igneous rocks from Jordan. Inst. App. Geol. (Jeddah) Bull., 3, 155-164.

Sigachev, S.P, Kopp, M.I, Elias, K., Hafez, A., Adzhamyan, Z.H., and Fakyani, F. (1995). Tectonic data for the Levant fault by using mesotectonic measures (Ghab and Missiaf areas). Geological Sciences Review, Damascus, 5, 75-81, (In Arabic).

Tarling, D.H., (1983). Palaeomagnetism, Chapman & Hall, London, pp.379.

Tarling, D. H. Sanver, M. and Hutchings A. M. J. (1967). Further palaeomagnetic results from the Federation of South Arabia. Earth Planet. Sci. Letters, 2, 148-154.

Torq, F. Besse, J., Vaslet, D., Marcoux, J., Ricou, L., E., Halawani, H., and Basahel, M. (1997). Palaeomagnetic results from Saudi Arabia and the Permo-Triassic Pangea configuration. Earth Planet, Sci. Letters, 148, 553- 567.

Trifonov, V.G., Trubikhin, V.M., Adzhamyan, Z., Dzhallad, S., El-Khair, Y. and Ayed, K. (1991). Levant fault zone in northwest Syria. Geotectonics, 25, 145-154.

Van Dongen, P.G., Van der Voo, R. and Raven, Th. (1967). Palaeomagnetic research in Central Lebanon Mountains and in the Tartous area (Syria). Tectonophysics, 4, 35-53.

Yousif, I. A. and Beckmann, G.E. (1981). A palaeomagnetic study of some Tertiary and Cretaceous rocks in western Saudi Arabia, evidence for the movement of the Arabian plate. Bull. Fac. Earth Sci. King Abdullaziz University, 4, 89-106.